Remote Sensing of Environment 208 (2018) 15–26

Contents lists available at ScienceDirect

Remote Sensing of Environment

journal homepage: www.elsevier.com/locate/rse

Coincident beach surveys using UAS, vehicle mounted and airborne laser scanner: Point cloud inter-comparison and effects of surface type heterogeneity on elevation accuracies

Paul Elsner[a,*], Uwe Dornbusch[b], Ian Thomas[c], Dan Amos[d], James Bovington[d], Diane Horn[a]

[a] Birkbeck, University of London, Department of Geography, Environment and Development Studies, Malet Street, London WC1E 7HX, UK
[b] Environment Agency, Worthing BN11 1LD, UK
[c] Pevensey Coastal Defence Ltd, Environment Agency Depot, Coast Road, Pevensey Bay, East Sussex BN24 6ND, UK
[d] Strategic Regional Coastal Monitoring Programme, Adur and Worthing Councils, Worthing Town Hall, Chapel Road, Worthing, West Sussex BN11 1HA, UK

ARTICLE INFO

Keywords:
UAS
UAV
Laser scanning
Beach monitoring
Accuracy analysis
LiDAR

ABSTRACT

Reliable and consistent topographic data is key to a multitude of environmental manangement and research applications. Unmanned Aerial Systems (UAS) are fast establishing themselves as a promising additional remote sensing platform that provides high spatial resolution not only of topography but also surface types and coastal features together with comparatively low costs and high deployment flexibility. However, comprehensive information on the accuracy of UAS-based elevation models in comparison to other available surveying methodology is regulary limited to be referenced to individual methods. This paper addresses this shortcoming by comparing coincident beach surveys of three different point cloud generating methods: ATV mounted mobile laser scan (MLS), airborne LiDAR (ALS), and UAS. This was complemented by two RTK-GPS surveys on a pole with wheel attachment and mounted on an ATV.

We present results in relation to elevation accuracies on a concrete control surface, the entire beach and for six different beach surface types together with how differences between point clouds propagate during the construction of gridded elevation models. Overall, UAS point cloud elevations were consistently higher than those of ALS (+0.063 m) and MLS (+0.087 m). However, these results for the entire beach mask larger and smaller differences related to the individual surface characteristics. For all surface types, UAS records higher (from 0.006 m for wet sand to 0.118 m for cobbles, average of 0.063 m) elevations than ALS. The MLS on the other hand, records predominantly lower elevation than ALS (−0.005 m for beach gravel to −0.089 m for soft mud, average of −0.025 m) except for cobbles, where elevations are 0.056 m higher.

The comparison shows that all point cloud methods produce elevations that are suitable for monitoring changes in beach topography in the context of operational coastal management applications. However, due to the systematic differences between respective monitoring approaches, care needs to be taken when analysing beach topographies for the same area based on different methods.

The eventual choice of monitoring method is therefore guided by a range of practical factors, including capital cost of the system and operating costs per survey area, conditions under which the system can operate, data processing time, and legal restrictions in the use of the system such as air safety regulations or limitation of ground access to areas with environmental protection.

1. Introduction

The high variability of natural environments such as beaches at a wide range of temporal and spatial scales in relation to, for example, topography and surface characteristics (Dornbusch et al., 2008; Watt et al., 2008) presents a substantial challenge to their monitoring. Historically, ground survey methods ranging from simple one person approaches (Delgado and Lloyd, 2004) to optical methods (Anderson et al., 1998) to GNSS point collection (Goncalves et al., 2012) have been used to monitor fixed profiles due to the time requirements to record individual points. The more rapid point acquisition using GNSS together with surface interpolation software has meant that different sampling strategies including mounting the receiver on vehicles such as All Terrain Vehicles (ATV) can be used to represent full 3D surfaces

* Corresponding author.
E-mail address: p.elsner@bbk.ac.uk (P. Elsner).

https://doi.org/10.1016/j.rse.2018.02.008
Received 31 December 2016; Received in revised form 6 February 2018; Accepted 8 February 2018

rather than individual profiles (Dornbusch, 2010). Recent developments also include the analysis of laser return intensity in the analysis and offer range novel applications of Lidar remote sensing beyond 3-D (Eitel et al., 2016).

Finally, advances in the field of Unmanned Aerial Systems (UAS) are now emerging as a promising additional remote sensing platform that provides high spatial resolution not only of topography but also surface characteristics and coastal features (Papakonstantinou et al., 2016). Since it is also comparatively low-cost and very flexible in terms of deployment (Mancini et al., 2013; Micheletti et al., 2015a; Nex and Remondino, 2014) it has as a consequence started to become the method of choice for some coastlines (Gonçalves and Henriques, 2015; Turner et al., 2016).

A central advantage of the UAS approach is that two data sets can be acquired at the same time: (i) multi-spectral data sets which capture information about the spatial distribution of surface characteristics such as the spatial distribution and patterns of sand and gravel at mixed beaches, and (ii) elevation models using novel photogrammetric approaches such as Structure-from-Motion (SFM) (Westoby et al., 2012) that relax many of the prerequisites of classical digital photogrammetry. The potential for the use of unmanned aerial systems for coastal monitoring has been recognised for a number of years and the use of UAS is becoming increasingly common (Brunier et al., 2016; Harwin and Lucieer, 2012; Klemas, 2015; Lim et al., 2015; Mancini et al., 2013; Pereira et al., 2009). However, comprehensive information on the accuracy of UAS-based elevation models in comparison to other available surveying methodology is limited. Reports of how UAS projects perform in operational circumstances against other surveying methods often only compare UAS-based elevation individually against those derived from Total Station (Harwin and Lucieer, 2012), RTK-GNSS (Gonçalves and Henriques, 2015; Turner et al., 2016), or laser scanning (Flener et al., 2013; Mancini et al., 2013). This paper aims to address this shortcoming by reporting for the first time comparisons of surveys of five different methods carried out within a one hour time window: three point cloud generating methods (ATV mounted mobile laser scan, airborne LIDAR and UAS), complemented by two line transects collected with a RTK-GNSS on a pole with wheel attachment and a RTK-GNSS mounted on an ATV. We present results in relation to elevation accuracy overall and for different surface characteristics. The implications of these results for are explored for both the construction of elevation models and planning and implementation for future scientific studies, particularly in the coastal management context.

2. Experimental set-up and methodology

2.1. Study site

The study was carried out covering an area of 65,500 m^2 along an approximately 450 m long stretch of the 9 km long shingle barrier at Pevensey Bay, East Sussex, UK (Fig. 1). The south-east facing beach is in a macrotidal environment with a mean spring tide range of over 6 m and an average annual maximum offshore wave height (0.05% exceedance) of ~4 m.

The beach profile at Pevensey can best be described as a composite mixed beach where the reflective upper beach (beach toe at approximately −1.5 m OD) is composed of mixed sand and gravel, fronted by a very shallow gradient, dissipative and mostly sand covered low-tide terrace (Watt et al., 2008) that in this location is underlain by intertidal back barrier sediments and sandstone over which the barrier has rolled back (Fig. 2). The surface sediment on the upper beach face can change over the course of a tide from a several decimetre thick pure gravel layer to a very hard surface layer of mixed sand and gravel with both types commonly found at the same time on different parts (cross-shore and longshore) of the beach (Dornbusch et al., 2008; Watt et al., 2008).

Pevensey Bay beach acts as a natural sea defence which provides protection from permanent flooding to an area of 50 km^2, most of which is significantly below high tide level. The beach is managed through recharge, reprofiling and recyling of sediment within the frontage. The field site was chosen because it represents are an example of a rapidly changing dynamic coastal environment that requires monitoring on a regular basis. It also exhibits a range of different surface types which makes it possible to investigate the influence surface variation on surveying accuracy. The presence of a nearby concrete outfall offered additionally the opportunity to calibrate measurements to such control surface.

Five concurrent surveys were carried out on the morning of May 20, 2015 during low water spring tide. These were:

a) Cross-shore beach transects collected with a wheel-based RTK-GNSS (W-GNSS):
The instrument set-up and survey strategy follows that described in Dornbusch (2010) using a 0.28 m diameter wheel attached to a 1.8 m high survey pole with a Leica 1200 sampling at 1 Hz (Fig. 3a). Walking speed and thus point density along the path was adjusted to the change in topography. This method relies on the contact with the beach surface and the constant distance between surface and GNSS receiver, so the main source of elevation errors comes from the GNSS sensor, but also from minor sinking in of the wheel on different sediment types (Fig. 2), pole non verticality and the surface wheel contact point moving away from vertically under the antenna on steeper slopes.
b) Longshore beach transects collected by ATV-based RTK-GNSS (ATV-GNSS):
Longshore transects were collected using a Trimble R8 receiver mounted on an ATV (Fig. 3b). Individual points were collected using Trimble's “Continuous Topo” mode, sampling at 1 Hz. The typical driving speed was 2.7–5.4 ms^{-1}. The receiver was mounted 1.4 m above ground level as close as possible to the front left wheel of the ATV, so that as long as the wheel stayed in contact with the beach, the receiver height was relevant. Data resulting from these surveys is processed through a bespoke software package developed by McCarthy Taylor Systems Ltd. which corrects for non-verticality of the mounting pole. Like the W-GNSS method it relies on the contact with the beach surface and constant distance between surface and GNSS receiver. ATV wheels do sink into the beach surface but this was somewhat limited due to very low pressure in the tyres. Nevertheless, on pure gravel the sinking distance could reach several centimetres, especially in curves (Fig. 2). In addition, the wheel suspension system introduces variations of the constant distance.
c) ATV-based mobile laser scanning (MLS):
The MLS set-up consisted of a single head MDL Dynascan Laser Scanning System (M250) including a laser scanning module (with a pulse rate of 36 kHz at 1200 rpm), an Inertial Measurement Unit (IMU) and two GNSS receivers for position and heading data mounted on an ATV (Fig. 3c). The instrument is mounted 2 m above the surface. The footprint of the laser on the ground changes rapidly with distance, but is generally in the order of 0.1 m at a distance of 50 m (Renishaw, 2016). The driving speed varied between 4 and 10 ms^{-1}. The MLS system is operated by the Worthing Borough Council Coastal Survey Team and has been used for routine beach surveys since 2013. The sinking in of the vehicle is similar to that for the ATV-GNSS (Fig. 2), but is of no consequence as beach elevation is measured relative to the GNSS position of the instrument.
d) Airborne laser scanning (ALS) on board a survey aircraft:
ALS data was collected by the Geomatics team of the UK Environment Agency using an Orion Airborne Laser Terrain Mapper flown on a Cessna 406 (G-LEAF, Fig. 3d). Flights were carried out at 900 m above ground at a speed of 260 kmh^{-1} with a scanning frequency of 40 kHz and a scan angle of 50°. Flight paths were parallel to the coast with an overlap of 30%. The survey covered the entire length of Pevensey Bay which included two ground control areas outside the study area.

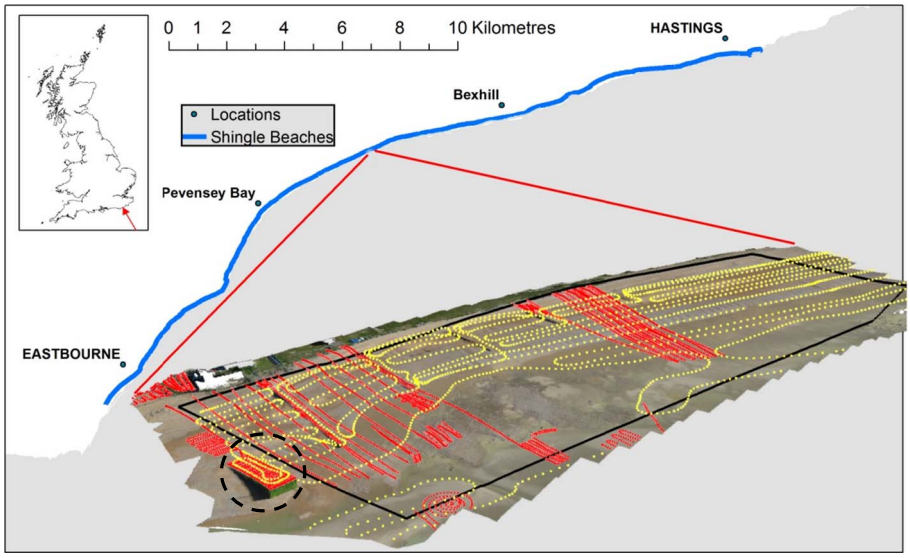

Fig. 1. Overview map and orthophoto of the study area, generated from UAS images. Yellow dots represent data collected with ATV-based RTK-GNSS, red dots represent data collected with pole-based RTK-GNSS. The black box outlines actual study area. Dashed circle depicts sluice outfall with concrete surface that was used as test surface. (For interpretation of the references to colour in this figure legend, the reader is referred to the web version of this article.)

Fig. 2. View down beach with the mixed beach in the foreground and the low tide terrace in the background. The two near parallel wheel traces are from the ATV_GNSS and were the first, the strongly curved one is from the MLS, which came second, and the thin line with foot prints going up the beach to its right in the centre of the photos are from the W-GNSS coming last.

The potential source of error for ALS measurements lies in the GNSS positioning of the plane, pitch, roll and yaw of the plane compensated through an IMU and adjustment of flightpaths against each other, laser measurement itself and the signal footprint of approximately 0.2 m diameter.

e) A multi-rotor UAS platform, represented by a Tarot 680Pro series Arducopter GNSS Hexacopter (Fig. 3e) carrying a Canon PowerShot A2300 16.0 megapixel camera. The copter was equipped with a Pixhawk flight controller and a GNSS module with compass. This allowed it to carry out pre-programmed autonomous survey missions using the software Mission Planner (Oborne, n.d.). The survey itself was carried out in autopilot mode during which the UAS flew at a height of approximately 70 m above ground, which resulted in a final data set of 145 images with a ground sampling distance (GSD) of 1.7 cm per pixel and a minimum overlap of 60% in both the side- and forward direction. The images were then processed using the SFM-based package Photoscan (Agisoft Photoscan, 2015). It performs an automatic camera calibration by estimating both internal and external camera orientation parameters, including nonlinear radial distortions based on the images EXIF meta data. Surface construction was carried out in a three step process, starting with image alignment by detecting and matching common feature points across images. The establishment of this basic geometric structure resulted in computed camera positions and a sparse point cloud. This was followed by the generation of a dense point cloud model, where the estimated camera positions were used to calculate depth information for each image which was then combined into a single dense point cloud for the entire surface. A number of quality settings were possible at this stage which essentially offered trade offs between accuracy and computing speed. For this project the *Ultra High* option was selected that ensured that the full photo resolution was utilised by the programme. The final step consisted of building a three dimensional polygonal model mesh, based on the previously generated dense point cloud and overlaying this with orthophoto texture which allowed the best visual representation of the generated 3D model.

For a more detailed description of Agisoft and its underlying principles, the reader is referred to (Gonçalves and Henriques, 2015). A bundle adjustment transformation was eventually carried out to reference the model to a British National Grid coordinate system using 49 ground control points, resulting in a vertical RMSE of the residuals of 4.6 cm. The control points had been surveyed with a Leica Viva GS08 RTK- GNSS receiver linked into the GNSS SmartNet Network RTK service. The points were placed on groins evenly spread across the study area, as these represent semi-permanent features that could be reused for subsequent surveys. This would mimic an approach that is likely to be taken in an operational surveying setting.

The W-GNSS transects resulted in 5613 points, and the transect surveyed with ATV-GNSS collected 2427 points, both shown in Fig. 1. The MLS point cloud of the study area consisted of 5.3 million points, equivalent of an average of 112 points/m^2. However, the density of the MLS point cloud varied substantially, with some sections of the foreshore being captured very sparsely (Fig. 4a), due to surface wetness where signal return away from the scanner deteriorated substantially. ALS collected 270,000 points within the case study area with a homogeneous distribution. This equalled a point density of approximately 4 points per m^2. The UAS-based surface model was generated using an

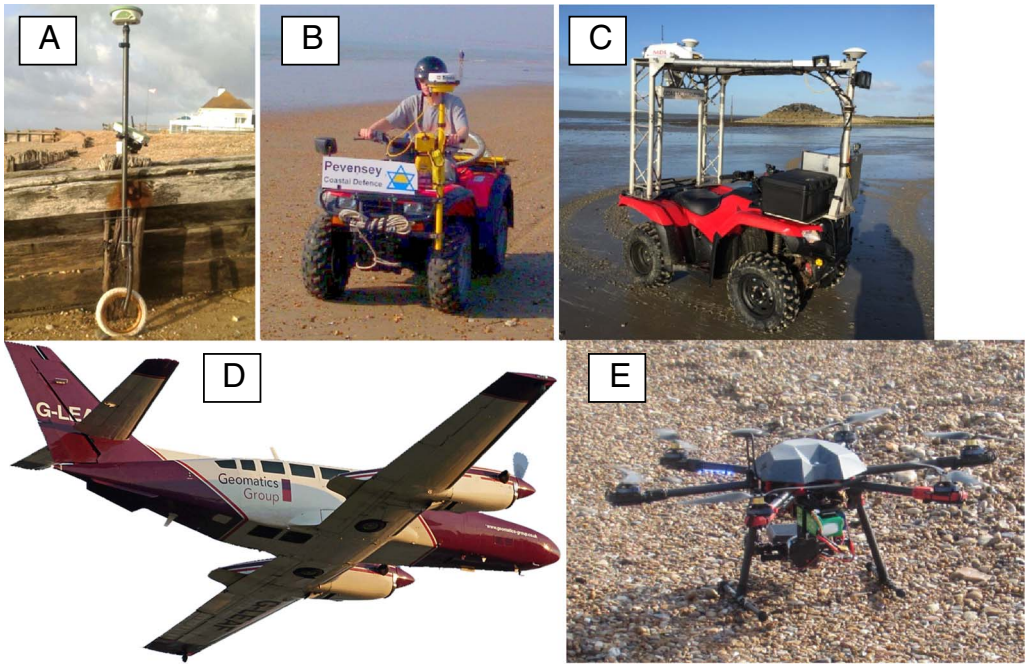

Fig. 3. Survey methods deployed concurrently at the study area: (A) wheel-based RTK-GNSS (W-GNSS), (B) ATV-based RTK-GNSS, (C) mobile laser scanning using sensors mounted on an ATV (MLS), (D) airborne laser scanning (ALS), and (E) multi-rotor UAS.

image overlap pattern where all parts of the study area were imaged from at least three perspectives and most of them by many more (Fig. 4b). The resulting point cloud had a homogeneous distribution and was represented by 3.8 million points within the study area. This translated into an average density of 58 points per m^2.

The central objective of this paper was to compare the elevation accuracy of the presently used methods of airborne laser scanning and terrestrial laser scanning with that of the new UAS-based surface modelling so that conclusions can be drawn for practical aspects of operational beach monitoring. This included the calculation of the root-mean-square error (RMSE):

$$RMSE = \sqrt{\frac{\sum_{i=1}^{n} (h_g - h_p)^2}{n}}$$

where h_g represents the height value measured by respective GNSS devices and h_p represents height value from respective point clouds.

The data analysis was carried out in a set of subsequent steps, consisting of (i) comparison of point cloud performance against W-GNSS and ATV-GNSS data collected on a concrete control surface; (ii) comparison of point cloud performance against both W-GNSS data and the ATV-GNSS on the actual beach study area; (iii) point cloud inter-comparison, including the consideration of different surface types; and (iv) an evaluation of differences between elevation models generated from the respective point clouds.

3. Results

3.1. Comparison of W-GNSS and ATV-GNSS data with point clouds

The relative elevation accuracy between RTK-GPS data and respective point clouds was first estimated on the homogeneous 30 m × 10 m concrete surface of a sluice outfall immediately to the west of the actual beach study area (see Fig. 1). Common point pairs for each data set combination were identified which were within a maximum distance of 0.2 m from each other. This was based on the assumption that, on the concrete surface, elevation differences between point pairs would be a function of survey methodology alone and not of actual changes of the surface over such a short distance.

The analysis started with a comparison using W-GNSS data which is taken as the most accurate due to the least number of error sources. Table 1 lists the satellite constellation conditions during the three phases of the W-GNSS survey, i.e. (i) a survey of the concrete test

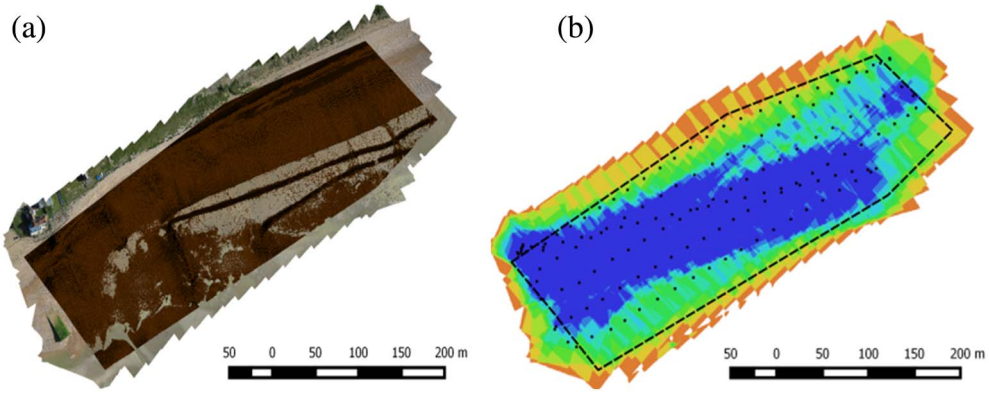

Fig. 4. Point cloud footprints generated by MLS (a) and camera locations and image overlap of the UAS survey (b). The dashed line outlines the actual study area.

Table 1
Satellite constellation conditions for the different phases of the W-GNSS survey, stating the range of geometric dilution of precision (GDOP), vertical dilution of precision (VDOP), horizontal dilution of precision (HDOP), and position dilution of precision (PDOP).

W-GNSS survey	GDOP	VDOP	HDOP	PDOP	Satellites used
Survey concrete test surface (start)	2.3–4.2	2.6–3.2	1.3–1.9	1.8–3.6	7 (GPS)
Survey study area	2.4–3.4	1.7–2.4	1.2–1.6	2.0–2.9	10 (GPS)
Survey concrete test surface (end)	2.3–4.1	1.6–3.0	1.1–1.6	1.9–3.4	9 (GPS)

surface surveying the study area; (ii) a subsequent survey of the study area itself; and (iii) a repeat survey of the concrete test surface at the end. It can be seen that all surveys experienced good conditions, with the study area itself experienced the most favourable and stable constellation with a geometric dilution of precision (GDOP) between 2.4 and 3.4.

Real-time kinematic (RTK) corrections of the GNSS measurements were carried out by utilizing a set of permanent and continuously operating OSNET reference stations. Six stations with a spacing of less than 70 km were used to develop a virtual reference station. The WGS84 reference system was used for all surveys.

The results of the accuracy analysis are displayed in Table 2. The best agreement was observed for the ALS point cloud elevation, where W-GNSS data was on average 0.016 m lower, with a RMSE error of 0.026 m and a standard deviation (STD) of 0.021 m. This comparison consists of two sets of W-GNSS data, one collected at the start of the survey and one collected 2 h later at the end of the survey, denoted “start” and “end” in Table 1. For the other comparisons this split is not shown. There is a 0.007 m systematic difference between the two data sets and a 0.01 m difference in the RMSE. The UAS-based point cloud showed a mildly higher difference of 0.023 m (RMSE 0.054 m and STD 0.049 m). The point cloud generated by ground-based mobile laser scanning exhibited the highest average difference with W-GNSS data being 0.072 m lower (RMSE 0.094 m, STD 0.061 m).

The analysis between ATV-GNSS and point clouds resulted in a similar pattern, with ALS data being the most consistent (average difference − 0.026 m, RMSE 0.038 m), followed by the UAS point cloud (average difference − 0.034 m, RMSE 0.074 m) and MLS points (average difference − 0.094 m, RMSE 0.107 m).

Finally, the accuracy of ATV-GNSS points was tested against the W-GNSS points, using the same approach as described above. This resulted in an excellent agreement with an average vertical difference of 0.005 m (RMSE 0.025 m), indicating that the two contact methods produced nearly identical results on the control surface (Table 2).

The second comparison of point cloud accuracy in reference to RTK-GNSS measurements was undertaken for the case study beach area itself including both W-GNSS and the ATV-GNSS data. For this analysis, only point groups within 0.1 m distance were employed, that is, a GNSS point was only used when all three point clouds had an elevation measurement within a radius of 0.1 m to the GNSS point. The reduction of the search distance was motivated by the fact that on the beach itself morphological changes occur over much shorter distances. For W-GNSS data, the ALS point cloud data again was the most accurate, both in terms of elevation difference (−0.0001 m) and RMSE (0.036 m). For the UAS point cloud data both the average error (−0.053 m) and RMSE (0.113 m) doubled in comparison to the concrete surface. MLS point cloud data had a smaller average error (−0.001 m) but a much higher RMSE of 0.145 m.

The results for the analysis using the ATV-GNSS as benchmark partly repeat the results for the M-GNSS in that the ALS point cloud had the smallest average error of −0.005 m (RMSE 0.036 m), the average error for the UAS point cloud doubled to −0.069 m (RMSE 0.108 m), whereas the average error for the MLS point cloud was lower with −0.011 m but the RMSE (0.113 m) was twice as high on the beach as on the concrete test surface.

3.2. Point cloud inter-comparison

The third step in the analysis focused on the vertical differences between respective point cloud data sets themselves. All point cloud analysis was carried out following an approach by Mancini et al. (2013) by developing a MATLAB© routine which identified common point groups where points from all data sets under investigation were identified that lay within a search circle radius of 0.1 m. This was based on the assumption that actual morphological vertical changes within this short distance can be considered to be minimal even on the beach. Any observed differences between data points could therefore be treated as a function of data acquisition methodology alone. The search routine identified 1960 matches. Groins and other man-made structures that could have had confounding influences were masked out.

The comparison of the two laser scanning point clouds shows a good agreement, with the MLS points being on average 0.025 m (RMSE 0.069 m) lower compared to the ALS data (see Fig. 5). The spatial distribution of the residuals shows a relative homogeneous distribution with a number of outliers being located along the eastern part of the foreshore.

The differences between UAS data and ALS data are shown in Fig. 6. UAS data exhibited on average higher elevations (+0.063 m) with a RMSE of 0.101 m. The spatial error pattern displays a cluster in the

Table 2
Difference of point cloud elevations as estimated against the contact methods for the concrete control surface and the beach study area, based on common points within a 0.2 m circle (concrete test surface) and 0.1 m (beach study area). Negative values for the average difference mean that the elevation of the GNSS method is lower than the respective point cloud. For example, in the first row, the W-GNSS elevations were on average 0.023 m lower than those of the UAS survey.

		Average difference (m)	RMSE (m)	STD (m)	Min (m)	Max (m)	Sample size
W-GNSS - UAS	Test surface	−0.023	0.054	0.049	−0.182	0.144	439
W-GNSS - MLS	Test surface	−0.072	0.094	0.061	−0.038	0.569	141
W-GNSS - ALS	Test surface	−0.016	0.026	0.021	−0.051	0.07	179
W-GNSS - ALS (start)	Test surface	−0.012	0.02	0.016	−0.031	0.053	95
W-GNSS - ALS (end)	Test surface	−0.019	0.03	0.02	−0.051	0.069	84
ATV-GNSS - UAS	Test surface	−0.034	0.074	0.066	−0.197	0.274	78
ATV-GNSS - MLS	Test surface	−0.094	0.107	0.053	0.027	0.244	19
ATV-GNSS - ALS	Test surface	−0.026	0.038	0.028	−0.014	0.082	22
W-GNSS - ATV-GNSS	Test surface	0.005	0.025	0.025	−0.064	0.043	29
W-GNSS - UAS	Study area	−0.053	0.113	0.1	−0.272	0.745	3567
W-GNSS - MLS	Study area	−0.001	0.145	0.145	−1.47	0.155	1772
W-GNSS - ALS	Study area	0.0001	0.036	0.036	−0.145	0.195	442
ATV-GNSS - UAS	Study area	−0.069	0.108	0.083	−0.225	0.683	1542
ATV-GNSS - MLS	Study area	−0.011	0.113	0.113	−1.809	1.153	881
ATV-GNSS - ALS	Study area	−0.005	0.036	0.036	−0.119	0.148	224

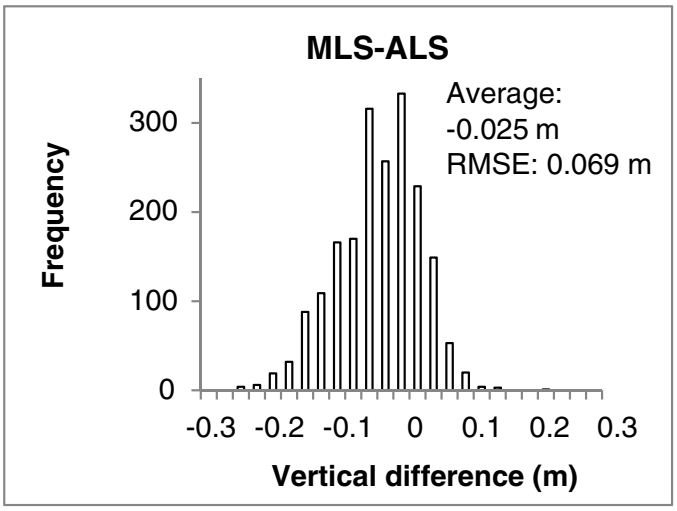

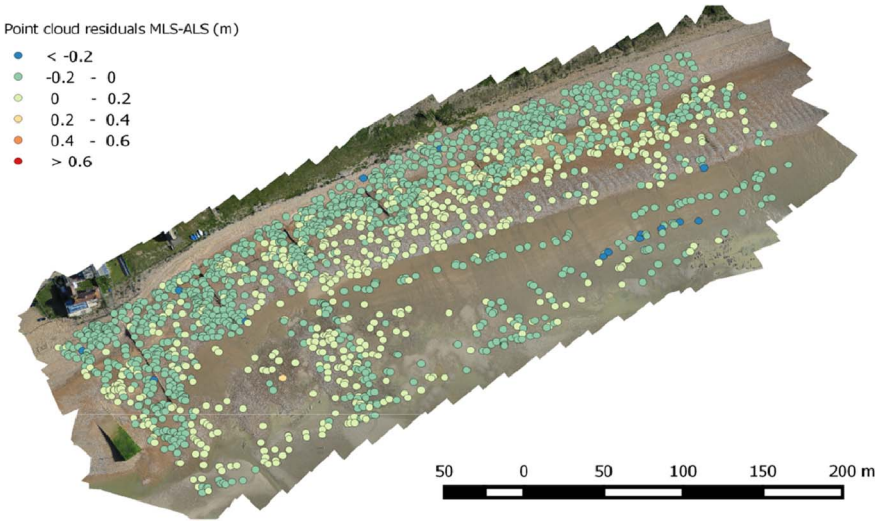

Fig. 5. Point cloud differences of MLS and ALS data (top), spatial distribution of residuals (bottom).

centre of the case study area where UAS elevations are lower than ALS points, whereas in other areas this was the opposite. In the south-western part of the study area on the upper shore there is a further small cluster of approximately 20 m by 20 m where UAS points are substantially higher. The reason for this was not fully clear but it is suggested that it be caused by a strong gust that disturbed the UAS platform in the respective flight line.

Fig. 7 illustrates the differences between UAS and MLS point clouds. It can be seen that the UAS-based point cloud has a positive offset of +0.087 m compared to the MLS data with a RMSE of 0.132 m. The spatial distribution of the errors shows a feature in the centre of the beach area with a cluster where UAS data was consistently lower than the MLS points, whereas in the other areas this was reversed.

As the study area exhibits a complex mix of surface types, the fourth comparison was carried out to evaluate to what extent surface variations had an effect on the measurement accuracy of the respective methods. This relates back to observations in Dornbusch (2010) where a difference between contact based GNSS and ALS data on concrete and pebble surfaces was observed. At the time of data acquisition, six different surface types and their locations were identified. These were: *beach gravel*, defined as sections of the upper beach that were homogenously covered with gravel (Fig. 2); *beach sand*, i.e. sections of the upper beach that had a homogeneous sandy surface; *cobble* is a section on the lower shore where a coarse lag deposit of larger clasts was exposed; *foreshore dry sand* marks areas of the lower foreshore that were slightly raised and where the sand surface had dried out, while *wet sand* describes areas of the lower foreshore where a thin film of water was still present on the surface during the surveys; *and soft mud* that relates to foreshore areas consisting of soft and muddy substrate. Fig. 8 shows the sections for which it was possible to visually outline the respective surface types with confidence from an orthophoto that was generated from the UAS images and field observations on the day.

The results of this analysis are shown in Fig. 9 with the sample size for the respective surface type being listed in Table 2. For all surface types, UAS records higher (from 0.006 m for wet sand to 0.118 m for cobbles, average of 0.063 m) elevations than ALS. The MLS on the other hand, records predominantly lower elevation than ALS (−0.005 m for beach gravel to −0.089 m for soft mud, average of −0.025 m) except for cobbles, where elevations are 0.056 m higher. The differences for gravel, which forms the dominant surface type, are much smaller for both UAS (0.038 m) and MLS (−0.005 m). Adjusting for the average difference and plotting the ALS-UAS and ALS-MLS difference, both UAS and MLS show similar patterns of differences to the ALS survey in relation to surface type. The cobble surface is the only one that shows much higher differences than the average for both UAS and MLS; the three sand surfaces are all below average as is the soft mud area. The

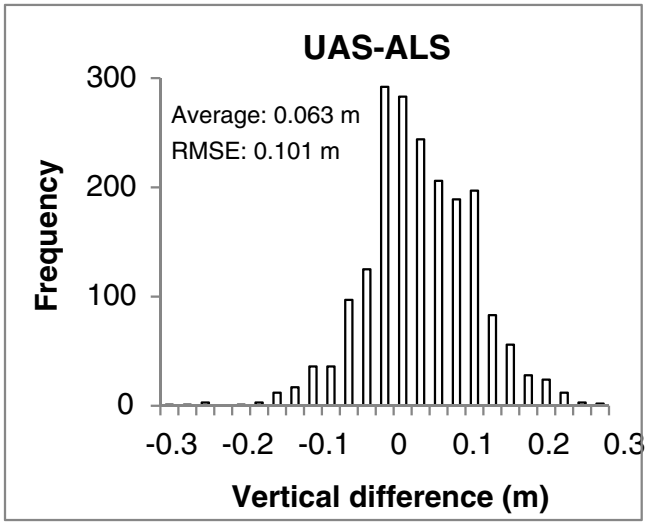

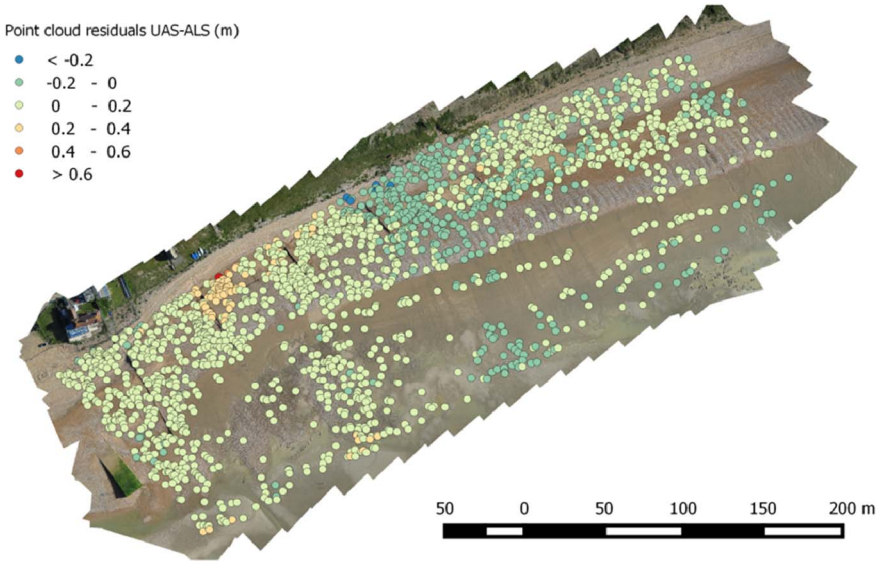

Fig. 6. Point cloud differences of UAS and ALS data (top), spatial distribution of residuals (bottom).

only slight exception is the gravel surface that is slightly above average for the MLS survey but slightly below average for the UAS survey.

3.3. Elevation model differences

In an operational coastal management context, survey point data are routinely converted to raster elevation models at pre-specified resolutions to identify areas of beach sediment loss or gain at different spatial scales and over different time periods. It is these data sets that are commonly analysed, visualised, and archived in digital formats that can be incorporated and shared across many GIS platforms. It is therefore important to understand how the observed differences in the primary point cloud data sets translate into interpolated raster elevation models. To do this, we generated raster DEM models from each of the point clouds in three spatial resolutions (0.2 m, 0.5 m, and 1 m), using the software package CloudCompare (Girardeau-Montaut, 2015). The height of each cell was determined by using the average height of all points falling in a grid cell. 'Empty' cells would be estimated by linear interpolation with the nearest non-empty neighbouring cells. This was particularly necessary for the MLS exhibiting substantial gaps in the foreshore region (Fig. 4). The differences between respective DEMs were analysed on a cell-by-cell basis and then aggregated.

Fig. 10 shows that the differences from the point cloud analysis is only replicated in the UAS-ALS relationship in that the average elevation difference is positive but slightly larger (0.07 m to 0.08 m for the different DEMs compared to 0.06 m for the point cloud). For the DEM difference between MLS and ALS, the negative difference of −0.02 m from the point cloud comparison changes to a positive difference of between 0.01 m to 0.05 m. There is also no obvious correlation between the magnitude of the difference and the cell size. In the case of UAS against MLS data, the average differences of elevation models were smaller than the original point cloud differences but showed no trend in terms of resolution.

4. Discussion

The results presented above show differences in elevation and calculated elevation models for the test beach which we will discuss in relation to the terrain, surface characteristics and survey methods.

All instruments used in this study rely on GNSS positions and elevations obtained during movement, that is no averaging during point occupation is possible. Dornbusch (2010) shows how elevations vary

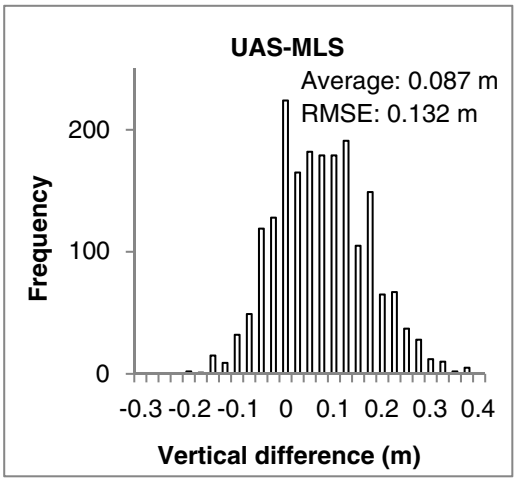

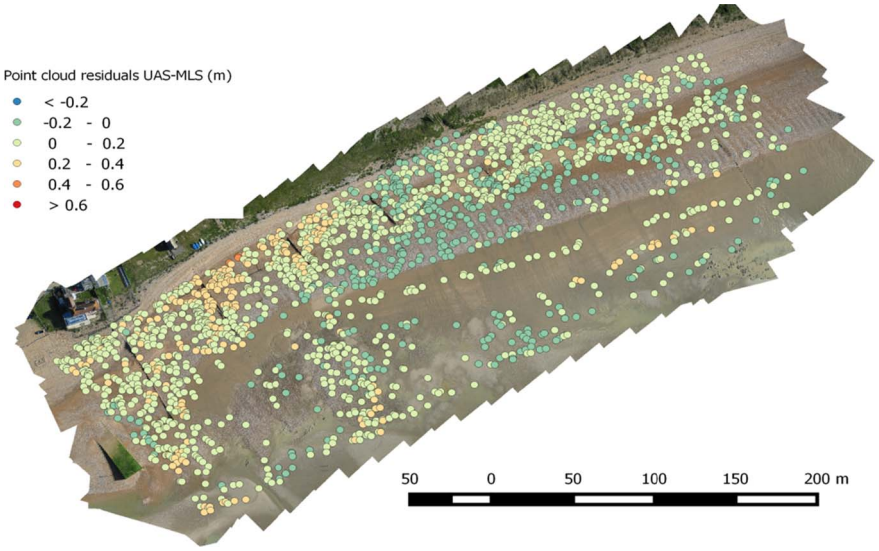

Fig. 7. Point cloud differences of UAS and MLS data (top), spatial distribution of residuals (bottom).

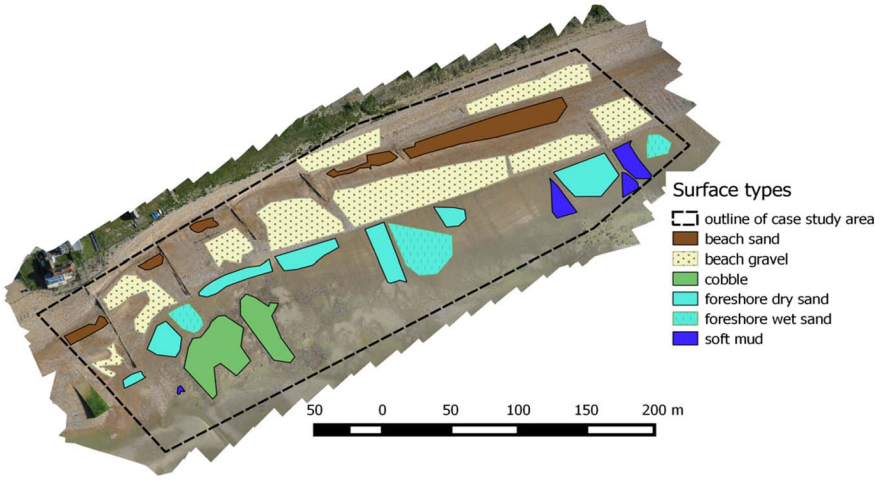

Fig. 8. Spatial distribution of surface types used for further analysis.

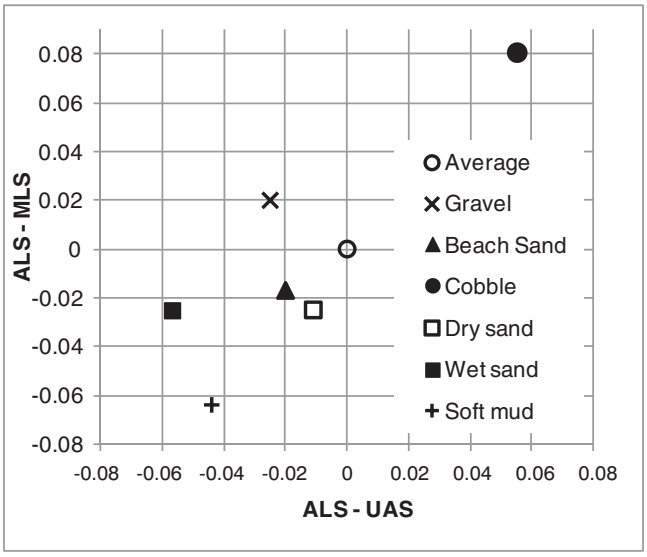

Fig. 9. ALS – UAS and ALS-MLS differences for different surface types from Table 2, adjusted for the beach average difference for both comparisons.

using the same W-GNSS approach used in the present study between surveys over different time scales. While the ALS and MLS elevations include measurements of the same surface at different times and thus provide some averaging of the GNSS signal, the W- and ATV-GNSS survey cover each surface only with one pass and are therefore more likely to include a GNSS bias. The only exception to this is the W-GNSS survey of the concrete outfall surface and the difference with ALS in Table 1 confirms a centimetre scale difference between the 'start' and 'end' surveys. The UAS method employed in this study relies on GCP points collected in static mode where GNSS averaging has taken place over 3 s. This means that any differences between surveys within approximately ± 0.01 to 0.02 m are very likely to be associated with the uncertainty in the GNSS system and that any difference between two methods associated with the whole method system have to be larger than this.

The comparison between the contact methods on the concrete test survey shows a very high degree of agreement for common points with the W-GNSS only 0.005 m higher than the ATV-GNSS (Table 1). This is based on 29 points that are within 0.2 m of each other. A very similar result with W-GNSS being 0.01 m higher than the ATV-GNSS is achieved by calculating the average elevation of the same surface using all 406 (W-GNSS) and 91 (ATV-GNSS) measurements taken. Given the general GNSS uncertainty, the two data GNSS sets can be treated as recording the same surface elevation on the concrete outfall and, given they consist of three different surveys in time, are assumed to represent the 'true' surface elevation. This also suggests that despite visible traces of sinking in of the ATV-GNSS system on the beach (Fig. 2), this has no measurable impact on overall elevations which also include areas with a firmer surface.

Comparison of ALS with both the GNSS surveys on the concrete shows small differences and the lowest RMSE values of the three contactless methods. This is evidence for the robustness of the survey grade ALS equipment and ideal conditions of the test surface in relation to the near vertical laser beam on the aircraft platform. The ALS – GNSS comparison on the beach surface (Table 1) also shows the best agreement in elevation and the lowest RMSE values.

To provide a more consistent comparison for all tests, Table 3 summarises all results in relation to the ALS survey as it is common to all comparisons including the point cloud only comparisons and provides the best representation of the true surface owing to the consistency and spatial homogeneity of the dataset.

On the concrete surface, the UAS data had a very low systematic error, but exhibited a wide scatter resulting in a higher RMSE. It is suggested that the low optical contrast of the surface (either clean concrete or with a cover of *enteromorpha* sp. algae, Fig. 11) is a possible reason for this, causing individual point errors in the image matching process that, however, eventually cancel each other out. The MLS data exhibits a systematic offset and RMSE outside of what could be expected from GNSS uncertainty. Inspecting the point cloud for the MLS data on the outfall (Fig. 11), it is apparent that the outfall test surface was only covered by one pass of the MLS ATV as it travelled in a northeast-southwest direction on the beach above the concrete surface, so that the point density changed significantly with distance over the concrete surface and the incidence angle became very shallow as the ATV moved down the beach. The average elevation of the outfall is 1.39 mOD which is reflected in the landward portion of the MLS data, but elevation increases with distance from the instrument seawards. This highlights that in contrast to ALS, where due to the flying height and scan angle the maximum angle between a horizontal surface and the laser beam is 25° with only a small difference in distance between instrument and surface along the swath, the incidence angle and distance on the MLS changes dramatically with every rotation of the scan

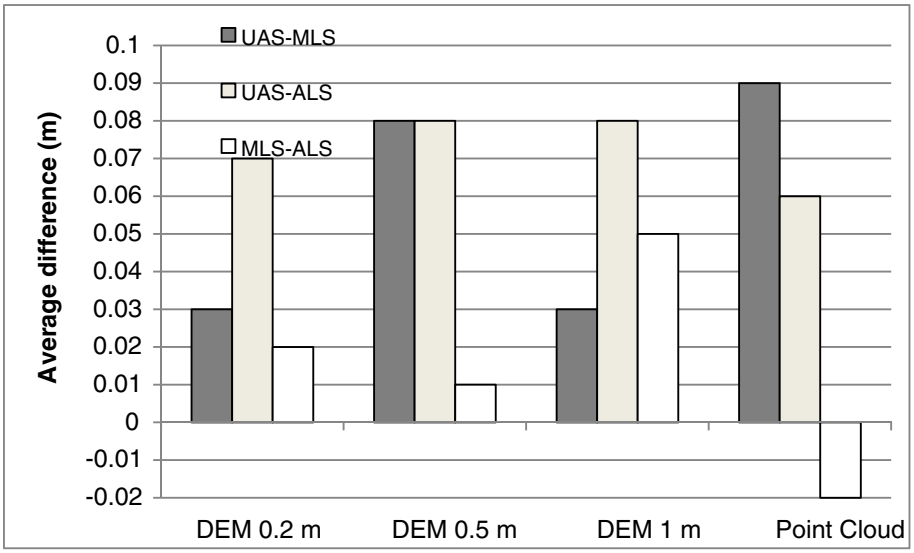

Fig. 10. Average differences of elevation models generated from respective point clouds. The error of the input point cloud is given for reference.

Table 3
Elevation differences from Table 2 and Fig. 5, 6 and 9 converted into elevation differences relative to ALS. Negative values mean that the method in the column heading was lower, positive that it was higher than ALS; for example, on the concrete surface the MLS data was on average 0.056 m higher than the ALS data using the W-GNSS comparison and 0.068 m higher using the ATV-GNSS comparison. For the point cloud comparison results of UAS and MLS, the RMSE value is also shown in parentheses. * indicates differences calculated indirectly for ATV and W-GNSS based on the ATV- and W-GNSS comparison on the concrete outfall of −0.026 m.

Elevation differences in m	UAS		MLS		W-GNSS	ATV-GNSS
ALS concrete (W-GNSS)	0.007		0.056		−0.016	−0.021*
ALS concrete (ATV-GNSS)	0.008		0.068		−0.021*	−0.026
ALS beach (W-GNSS)	0.0531		0.011		0.0001	−0.0049*
ALS beach (ATV-GNSS)	0.064		0.006		0*	−0.005
ALS beach cloud (Fig. 5, 6 and 9)	0.063	(0.101)	−0.025	(0.069)	–	–
Gravel	0.038	(0.087)	−0.005	(0.063)		
Beach sand	0.043	(0.08)	−0.042	(0.07)		
Cobble	0.118	(0.0.123)	0.056	(0.088)		
Dry sand	0.052	(0.072)	−0.05	(0.083)		
Wet sand	0.006	(0.073)	−0.05	(0.076)		
Soft mud	0.019	(0.072)	−0.089	(0.122)		
DEM 0.2 m grid	0.07		0.02			
DEM 0.5 m grid	0.08		0.01			
DEM 1 m grid	0.08		0.05			

head. This is generally compensated for in the data processing by combining the data from several passes across the same area from different angles but in the case of a single pass over a smooth and partly moist surface at a shallow angle, the results are not very reliable.

The analysis comparing point cloud data against RTK-GNSS data on the actual beach area introduces additional error sources due to the interaction between the surface and the equipment, and the timing of the surveys. The contact based methods (W-GNSS and ATV-GNSS) are shown to sink into the surface of the study area depending on the type of surface and the weight of the equipment; surface micro topography increases from a smooth sand surface to a sand surface with ripples to gravel to cobbles; wet sand provides a different reflectivity to dry surfaces and the sequence in which the surveys were carried out meant that the contactless methods picked up at least some of the traces left by the contact methods and the MLS (Fig. 2). Further to the surface roughness, the surface porosity changes and while the contact methods record the highest points of the surface (albeit this is possibly over-compensated for by the sinking in), the MLS with its laser footprint in the millimetre to centimetre range will return an elevation that is a composite but possibly be slightly below a surface of the highest points.

The comparisons on the beach in Table 3 show again how close ALS and the two GNSS methods are with negligible differences and RMSE values of 0.03 m and 0.036 m only about 0.01 m higher than on the concrete surface (Table 2). The comparison also confirms indirectly (because there were no common points between W-GNSS and ATV-GNSS within 0.1 m on the beach) the high degree of agreement found between both contact methods on the concrete surface. It also suggests that the visible sinking in of the ATV-GNSS does not seem to impact the surface elevation. While the MLS data is significantly higher on the concrete outfall surface it is very close to the ALS on the entire beach, being only 0.011 m (based on the W-GNSS comparison) and 0.006 m (based on the ATV-GNSS comparison) higher. However, while the multiple paths covering each part of the beach serve to bring the average closer to the true surface, the inherent uncertainty of each individual point measurement results in a very high RMSE of 0.145 m and 0.113 m for the W-GNSS and ATV-GNSS comparisons, respectively.

In contrast to the MLS data, the UAS data shows very little systematic difference on the concrete surface but a significant difference on the overall beach of 0.0531 m and 0.064 m (RMSE values of 0.113 m 0.108 m) in relation to the W-GNSS and ATV-GNSS comparisons,

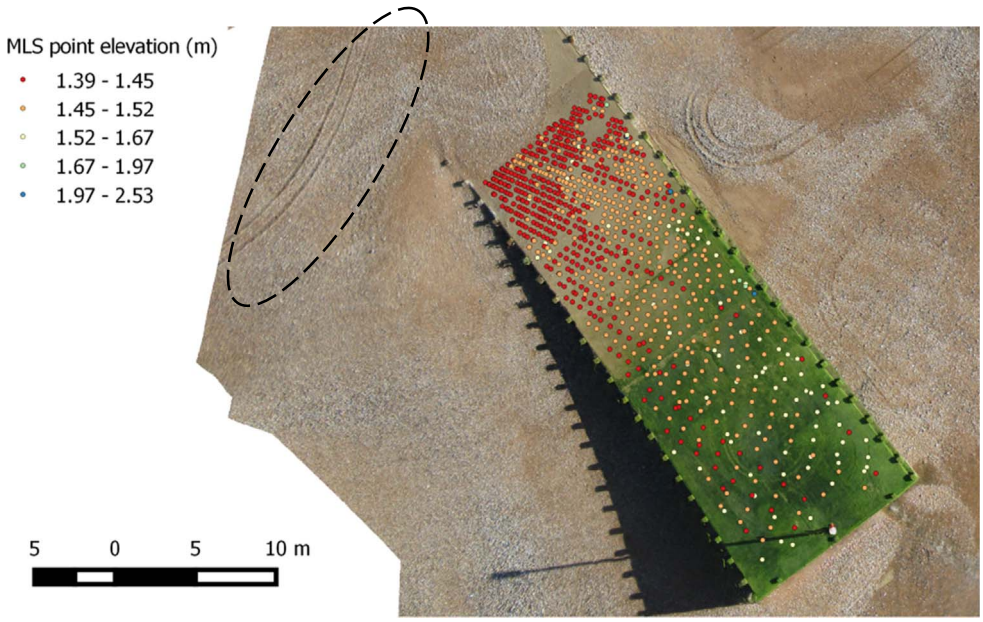

Fig. 11. Footprint of the mobile laser scanner (MLS) data on the concrete test surface of the sluice outfall, with dense regular pattern at landward end and increasingly lower resolution towards the seaward end. Ellipse in the top left highlights the track of the ATV carrying the laser scanner.

respectively.

Other than the comparison using the two GNSS surveys, where common points only exist for the comparison pair with the 0.1 m radius, the point cloud comparison is based on common points for all three point clouds within the 0.1 m radius resulting in 1960 point groups (Fig. 9). This point cloud comparison results in a very similar difference compared to that based on the GNSS surveys for ALS and UAS (systematic offset of 0.063 m) but for the MLS comparison a previously subtle positive offset changes to an overall negative offset of −0.025 m that falls outside of what is attributable to GNSS uncertainty and as this was not picked up in any of the other comparisons appears to be an offset due to the MLS method. Breaking down the overall beach into different surface components provides additional insight. The areas identified as belonging to a certain surface type taken together are smaller than the entire beach area (Fig. 8 and Table 3) with the remaining area not identified nevertheless belonging predominantly to the 'gravel', 'beach sand', 'dry sand' and 'wet sand' types. As a consequence, these types contribute a large part of the offset. For the UAS data, these types have a lower offset than the total beach which is disproportionally influenced by the relatively small areas of 'Cobble' which have a 0.118 m offset to the ALS data. Given the different size of ALS and UAS point footprint, ALS will inevitably provide a more averaged elevation while feature matching of the UAS method will pick up the individual cobbles, thus giving a higher elevation. This interpretation also applies to the MLS data where the general negative difference changes to a large positive difference, suggesting that the MLS is also picking out the cobbles rather than the lower areas between them. Overall, the comparison for different surface types appears to influence the elevation measurements although the number of sample points is quite low for the smaller surface types. For the MLS survey it would appear as if surfaces with higher roughness and thus good returns even on shallow incident angles of the laser beam, like gravel, produce elevations similar to ALS and GNSS, whereas smoother surfaces result in lower elevations or no returns (Fig. 4a). The MLS records the same differences for wet and dry sand which is most likely due to the fact that the MLS survey was carried out about 1 h before the UAS flight used to identify the different sand type areas, at which point previously wet sand had dried off in the early morning sun. This means that the MLS survey encountered the sand on the low tide terrace when it was still wet while the UAS survey was presented with distinct surface types, highlighting the importance of timing in relation to survey type and results.

The spatial pattern of residuals in the UAS – ALS comparison in Fig. 7, also seen in the UAS-MLS comparison, show on closer inspection of the UAS surface model that two images for that part of the beach had sub-optimal lighting which resulted in lower contrast. This apparently caused a localised problem for the elevation model of the SfM modelling process. Such problems have also been described by Flener et al. (2013). This issue illustrates a more general weakness of photogrammetry-based UAV methods. Surfaces with a heterogeneous and distinct texture are particularly well suited for a successful and efficient image matching process (Baltsavias, 1999). Reflective and/or homogeneous surfaces, however, are a more problematic challenge for the feature matching stage, leading to a higher numbers of erroneous outliers (Agisoft Photoscan, 2015; Fonstad et al., 2013). Surfaces such as concrete, sand, mud or gravel are examples of such optical homogeneity and are therefore challenging for SFM approaches. This might explain the relatively modest performance of the UAV point cloud when validated to GNSS measurements. In favourable conditions, the RMSE of SFM-based point clouds can be expected to be in the range of 1–2 multiples of the GSD. In the on-hand project, the RMSE was 3 GSD concrete test surface and 6–7 GSD on the study area. This corresponds to the performance of other coastal applications such as a UAV survey of beach dune systems where the GSD multiple of the RMSE was even higher (Mancini et al., 2013).

Some authors recommend therefore to avoid potentially challenging surfaces in SFM-based monitoring altogether (Micheletti et al., 2015b). However, this is often not practical in the operational monitoring context. Instead, users need to aware that less confidence can be placed in the results of optically problematic surfaces. An interesting method to address this problem is the addition of a near-infrared (NIR) channel to the UAV sensor, as was done in the context of snow monitoring (Bühler et al., 2017). This led to a significantly better performance during the image matching process. Such an approach might also be promising in the coastal context.

When it comes to gridding the data into DEMs, the UAS-ALS difference from the point comparison (0.063 m) translates into slightly higher positive values of 0.007 m to 0.008 m, irrespective of the grid size. In contrast, the small negative difference between MLS and ALS transforms into a positive difference of between 0.01 m and 0.05 m. The most likely reason for this is that significant shore-parallel areas of the low tide terrace have no MLS data (Fig. 4a) and so the interpolation starts from the shingle beach toe. Depending on the grid size and grid position, this last elevation for the beach around the beach toe is likely to be higher than the elevation of the low tide terrace just seawards of the beach toe leading to a large area of interpolated higher surface. The irregular intersection between the rectilinear grid and the slightly oblique running beach toe is likely to create the non-linear increase in average elevation, but the general increase of the 1 m grid over the other two is consistent, as the average elevation from points in a larger grid size on a slope will result in a higher elevation for that grid cell.

5. Conclusion

This work presents, to the best knowledge of the authors, the first comparison of UAS, MLS and ALS data collected at the same time on the same beach together with two GNSS methods to provide additional ground reference data. The results indicate that ALS is overall the most robust method owing to its maturity reflected in high instrument specification and long established and perfected flight planning and post processing as well as optimum orientation between instrument and object with relatively low incident angles. Bringing a laser scanner close to the ground as in the MLS increases the incidence angle with the surface dramatically, resulting in poorer reflection and, as a consequence, a much wider scatter of the data. Adding to this, the additional error terms associated with the GNSS and IMU on a fast moving vehicle over uneven ground produce the highest RMSE. Apart from on the concrete control surface, UAS elevations were consistently higher than ALS and, as a consequence the true surface elevation, by about 0.05 m with RMSE values about halfway between ALS and MLS. Individual spatial patterns of larger or smaller differences than the average appear to be related to sediment characteristics with some more suited, for example, to the pattern recognition of the UAS method or the better reflectivity of oblique incident laser pulses, while others create more difficulty due to surface homogeneity or poor reflectivity.

Generally, the more instruments or processes and the less time available to produce the co-ordinate, the larger the RMSE. This is illustrated by the low RMSE for the GNSS instruments sampling at 1 Hz which increases for the UAS due to uncertainties of the camera and image quality influenced by lighting conditions, inferred camera position, image matching and co-ordinate calculation in addition to the overall geo-referencing using GNSS as ground control or on board. The MLS has the highest RMSE despite only using three instruments (GNSS, laser, IMU). The speed of movement of the instrument comparatively close to the surface it is measuring together with the shallow angle of incidence lead to large point density but also high uncertainty as regards the location of each individual point.

The ALS system has the same number of components as the MLS, but the much smaller RMSE is a result of the more stable platform, more favourable position of the more sophisticated instrument in relation to the measured object. However, this also comes with significantly higher investment and operating costs.

The comparison shows that all methods produce elevations that can be used for operational monitoring beach topography changes. This means that UAS represent a viable, low cost and flexible alternative to laser scanning approaches. In addition to this, UAS have the added advantage that they collect multi-spectral image information about the surface under investigation. This secondary data set that can be used to, e.g. analyse the distribution of sand and gravel sections of the upper beach at Pevensey Bay.

However, when monitoring the same beach repeatedly, care needs to be taken to ensure that the data collected is sufficient for later analysis. In the case of UAS, the number of overlapping images needs to be extended beyond the actual area of the survey to avoid any edge effects from insufficient overlap creeping into the survey area. In addition, data quality (in this case the image quality analogue to the PDOP on GNSS equipment) must be checked during capture so that it can be reflown immediately if the quality is not satisfactory. In the case of the MLS, it requires ensuring that the same area is covered by several passes with different incident angles and recognising that some surfaces like wet sand may not produce a return even in close proximity to the scanner.

Given that in terms of accuracy all methods produce comparable results, the choice of UAS as operational monitoring method is likely to be guided by practical considerations:

- cost of the survey (capital cost of the system and operating costs per survey area),
- conditions under which the system can operate (e.g. wind, light levels, visibility despite clouds, fog or sea spray in the air),
- size and shape of the survey area and time window available for the survey,
- ease of calling off the system for a survey,
- processing time between the survey and the data becoming available,
- restrictions in the use of the system (e.g. regulations relating to airborne systems or ground access to areas with environmental protection),
- additional benefits such as orthophoto creation, surface type analysis or coincident use of other instruments (for example infrared cameras),
- required accuracy for smaller sub areas or
- point density.

Some of these factors will depend on the UAS platform, as rotary and fixed wing set-ups have different sensitivities to wind conditions shape of the survey area, or flying speed. Of further importance is the country it is used in, and its regulations on UAS use. The weighting of each of these factors will depend on the monitoring project and its objectives. UAS will in many cases be the method of choice, but as with every new method, especially if it replaces another method used to create data for the same location before, tests about comparability of the data collected with both methodologies are essential.

Some monitoring projects, like the English Network of Coastal Monitoring Programmes covers the same coastline with different methods at different times such as ATV-GNSS, MLS, ALS and static terrestrial laser scanning. As the research reported here demonstrates, there can be systematic differences between respective monitoring approaches. This means when a mix of survey methods is used, a better understanding of such effects is necessary and future research should investigate more systematically such sensitivities on e.g. the calculation of beach volumes differences.

Acknowledgements

The authors would like to thank the Geomatics team of the Environment Agency and Worthing Borough Council for their co-operation in survey scheduling and the supply of laser scanning data. Paul Elsner gratefully acknowledges Harriet Smith at SSHP Birkbeck for her continued support for the acquisition and maintenance of the GEDS UAS unit.

References

Agisoft Photoscan, 2015. Agisoft Photoscan User Manual - Optimisation. Version 1.2.3.
Anderson, J.M., Anderson, J.M., Mikhail, E.M., 1998. Surveying, Theory and Practice. McGraw-Hill Science/Engineering/Math.
Baltsavias, E., 1999. A comparision between photogrammetry and laser scanning. ISPRS J. Photogramm. Remote Sens. 54, 83–94.
Brunier, G., Fleury, J., Anthony, E.J., Gardel, A., Dussouillez, P., 2016. Close-range airborne structure-from-motion photogrammetry for high-resolution beach morphometric surveys: examples from an embayed rotating beach. Geomorphology 261, 76–88. http://dx.doi.org/10.1016/j.geomorph.2016.02.025.
Bühler, Y., Adams, M.S., Stoffel, A., Boesch, R., 2017. Photogrammetric reconstruction of homogenous snow surfaces in alpine terrain applying near-infrared UAS imagery. Int. J. Remote Sens. 38, 3135–3158. http://dx.doi.org/10.1080/01431161.2016.1275060.
Delgado, I., Lloyd, G., 2004. A simple low cost method for one-person beach profiling. J. Coast. Res. 20, 1246–1252.
Dornbusch, U., 2010. Ground survey methods for mixed sand and gravel beaches in intertidal environments: a comparison. J. Coast. Res. 26, 451–464. http://dx.doi.org/10.2112/08-1134.1.
Dornbusch, U., Robinson, D., Moses, C., Williams, R.B., 2008. Variation in beach behaviour in relation to groyne spacing and groyne type for mixed sand and gravel beaches, Saltdean, UK. Z. Geomorphol. 52, 125–143.
Eitel, J.U.H., Höfle, B., Vierling, L.A., Abellán, A., Asner, G.P., Deems, J.S., Glennie, C.L., Joerg, P.C., LeWinter, A.L., Magney, T.S., Mandlburger, G., Morton, D.C., Müller, J., Vierling, K.T., 2016. Beyond 3-D: the new spectrum of lidar applications for earth and ecological sciences. Remote Sens. Environ. 186, 372–392. http://dx.doi.org/10.1016/j.rse.2016.08.018.
Flener, C., Vaaja, M., Jaakkola, A., Krooks, A., Kaartinen, H., Kukko, A., Kasvi, E., Hyyppä, H., Hyyppä, J., Alho, P., 2013. Seamless mapping of river channels at high resolution using mobile liDAR and UAV-photography. Remote Sens. 5, 6382–6407. http://dx.doi.org/10.3390/rs5126382.
Fonstad, M.A., Dietrich, J.T., Courville, B.C., Jensen, J.L., Carbonneau, P.E., 2013. Topographic structure from motion: a new development in photogrammetric measurement. Earth Surf. Process. Landf. 38, 421–430. http://dx.doi.org/10.1002/esp.3366.
Girardeau-Montaut, D., 2015. CloudCompare Version 2.6.1. User Manual 181.
Gonçalves, J.A., Henriques, R., 2015. UAV photogrammetry for topographic monitoring of coastal areas. ISPRS J. Photogramm. Remote Sens. 104, 101–111. http://dx.doi.org/10.1016/j.isprsjprs.2015.02.009.
Goncalves, R.M., Awange, J., Krueger, C.P., 2012. GNSS-based monitoring and mapping of shoreline position in support of planning and management of Matinhos/PR (Brazil). J. Glob. Position. Syst. 11, 156–168.
Harwin, S., Lucieer, A., 2012. Assessing the accuracy of georeferenced point clouds produced via multi-view stereopsis from unmanned aerial vehicle (UAV) imagery. Remote Sens. 4, 1573–1599.
Klemas, V.V., 2015. Coastal and environmental remote sensing from unmanned aerial vehicles: an overview. J. Coast. Res. 31, 1260–1267.
Lim, M., Dunning, S.A., Burke, M., King, H., King, N., 2015. Quantification and implications of change in organic carbon bearing coastal dune cliffs: a multiscale analysis from the Northumberland coast, UK. Remote Sens. Environ. 163, 1–12. http://dx.doi.org/10.1016/j.rse.2015.01.034.
Mancini, F., Dubbini, M., Gattelli, M., Stecchi, F., Fabbri, S., Gabbianelli, G., 2013. Using unmanned aerial vehicles (UAV) for high-resolution reconstruction of topography: the structure from motion approach on coastal environments. Remote Sens. 5, 6880–6898. http://dx.doi.org/10.3390/rs5126880.
Micheletti, N., Chandler, J.H., Lane, S.N., 2015a. Investigating the geomorphological potential of freely available and accessible structure-from-motion photogrammetry using a smartphone. Earth Surf. Process. Landf. 40, 473–486. http://dx.doi.org/10.1002/esp.3648.
Micheletti, N., Chandler, J.H., Lane, S.N., 2015b. Structure from motion (SfM) photogrammetry. Geomorphol. Tech. 2, 1–12. http://dx.doi.org/10.5194/isprsarchives-XL-5-W4-37-2015.
Nex, F., Remondino, F., 2014. UAV for 3D mapping applications: a review. Appl. Geomatics 6, 1–15. http://dx.doi.org/10.1007/s12518-013-0120-x.
Oborne, M., n.d. Mission Planner Overview | Mission Planner [WWW Document]. URL http://planner.ardupilot.com/wiki/mission-planner-overview/ (accessed 3.8.16).
Papakonstantinou, A., Topouzelis, K., Pavlogeorgatos, G., 2016. Coastline zones identification and 3D coastal mapping using UAV spatial data. ISPRS Int. J. Geo-Information 5, 75. http://dx.doi.org/10.3390/ijgi5060075.
Pereira, E., Bencatel, R., Correia, J., Félix, L., Gonçalves, G., Morgado, J., Sousa, J., 2009. Unmanned air vehicles for coastal and environmental research. J. Coast. Res. 1557–1561.
Renishaw, 2016. Data Sheet: Dynascan M250.
Turner, I.L., Harley, M.D., Drummond, C.D., 2016. UAVs for coastal surveying. Coast. Eng. 114, 19–24. http://dx.doi.org/10.1016/j.coastaleng.2016.03.011.
Watt, T., Robinson, D., Moses, C., Dornbusch, U., 2008. Patterns of surface sediment grain size distribution under the influence of varying wave conditions on a mixed sediment beach at Pevensey Bay, southeast England. Z. Geomorphol. Suppl. 52, 63–77.
Westoby, M.J., Brasington, J., Glasser, N.F., Hambrey, M.J., Reynolds, J.M., 2012. "Structure-from-motion" photogrammetry: a low-cost, effective tool for geoscience applications. Geomorphology 179, 300–314. http://dx.doi.org/10.1016/j.geomorph.2012.08.021.